Mechanics of Advanced Composite Structures 7 (2020) 121 - 127

Mechanics of Advanced Composite Structures

journal homepage: http://MACS.journals.semnan.ac.ir

Semnan University

Elastic analysis of Shrink-fitted Thick FGM Cylinders Based on Linear Plane Elasticity Theory

M.R. Salehi Kolahi, M. Karamooz, H. Rahmani *

Department of Mechanical Engineering, University of Sistan and Baluchestan, Zahedan,Iran

PAPER INFO

FGM
Plane elasticity
Shrink-fit
Thick-walled cylinder

ABSTRACT

Nowadays, functionally graded materials (FGM) are widely used in many industrial, aerospace and military fields. On the other hand, the interest in the use of shrink-fitted assemblies is increasing for designing composite tubes, high-pressure vessels, rectors and tanks. Although extensive researches exist on thick-walled cylindrical shells, not many researches have been done on shrink-fitted thick FGM cylinders. In this paper, an analytical formulation for shrink-fitted of axisymmetric thick-walled FGM cylinders based on the linear plane elasticity theory is presented. The stresses and displacement fields in thick cylindrical shells are calculated using the real, Repeated and complex roots of characteristic equation. The displacements and stresses resulted are depicted for a case study. The results show that the material composition variation had evident effects on shrink-fit pressure in the intersection area of two fitted tubes. The value of this pressure affects radial and hoop stress distribution in FG circular cylinders walls.

1. Introduction

Functionally Graded Materials (FGMs) are advanced composite materials in which two or more different material ingredients change continuously and gradually. This results in elimination of interface problems, and consequently, uniformity of stress and temperature distribution. FGM materials are made from ceramic and metal. Usually, the composition varies from a ceramic surface to a metal surface. These changes are considered as power or exponential functions in the thickness directions [1-3].

To date many theorists and practitioners have intensively studied shell structures (e.g., cylindrical, spherical, etc.). Axisymmetric thick-walled cylindrical shells are common structural elements in many engineering applications, including pressure vessels, submarine hulls, rocket chambers, fuel storage tanks and many other structures. In order to optimize the weight, mechanical strength, displacement and stress distribution of a shell structure one approach is to use shells with functionally graded materials [4-8].

Shrink fitting is a process in which an interference fit is achieved by a relative size change after assembly. This is usually achieved by heating or cooling one component before assembly and allowing it to return to the ambient temperature after assembly [9, 10]. Heating the outer part may take a long time, and in some cases metallurgical reasons may prevent heating altogether. However, cooling the inner part will not affect the property of the material, and can be achieved much faster. Shrink fitting is a method used in making mechanical joints when axles, bushings and similar are to be fitted inside a part with a hole. Shrink-fitting is an effective way of assembling machine elements such as a gear to a shaft to transmit torque. In addition, shrink-fitted assemblies are widely used for steel rolling in the production of I-beams and rail sections. The advantage of a shrink-fitted assembly is that it is simple to manufacture, has high integrity and is capable of being subject to high loads. Shrink fitting of layered cylinders is a way of extending the fatigue lifetimes [11-15].

In 1852 for the first time, lame' proposed the exact solution of axisymmetric thick-walled cylindrical shells made of homogeneous and Isotropic material [16]. He used plain elasticity theory to obtain the stress distribution.

* Corresponding author. Tel.: +98-54-31132378
E-mail address: h_rahmani@eng.usb.ac.ir

DOI: 10.22075/MACS.2019.18551.1221
Received 2019-08-28; Received in revised form 2019-10-05; Accepted 2019-10-24

Lechnitsky in 1950 formulated the elasticity theory of composite structures [17]. In 1984, Niino et al. presented the concepts of FGM materials [18]. In 2006 Hongjun et al. derived the exact solution of FGM hollow cylinders in the state of plane strain with exponential function of elasticity modulus along the thickness of the cylinder [8]. In 2012, Ghannad and Zamani Nejad proposed a complete elastic solution of pressurized thick cylindrical shells made of heterogeneous FG materials [6]. They used plane elasticity theory. In 2018, Pourasghar et al. analyzed the three-dimensional thermoelastic deformation of FGM cylindrical shells subjected to thermal load [19].

During the past years, many scholars have studied the stress and strain distributions in hollow cylindrical shells made of FG materials but to the best of our knowledge, there is no complete analytical formulation for shrink-fitted thick FGM cylinders with a power variation of material properties. In 2006, Jehed et al. [13] studied the fatigue life time of multi-layer shrink-fitted cylinders made of homogenous materials. In 2012, Sharifi et al. investigated optimum design of shrink-fit multi-layer compound cylinders made of homogenous materials employing an analytical method [15]. In 2015, Arslan and Mack [20] presented an analytical formulation for rotating shrink fitted cylinders with considering thermal effects. In their study the outer cylinder is made of FG material and the inner part is a homogenous shaft. They only considered the real distinct roots of the characteristic function. In 2017, Apatay et al. [21] investigated elastic–plastic design of a rotating shrink fit with functionally graded hub using semi-analytical formulation. Motivated by the aforementioned remarks the focus of this research is to develop a complete analytical formulation for the behavior of shrink-fitted thick FGM cylinders based on linear plain elasticity theory. The final formulation is a closed-form solution of the differential equations therefore a purely analytical discussion of the problem is possible. The presented formulation is general as it considers all the possible roots of the characteristic function. So it can be used for any grading index and any end boundary condition. The remaining of this article is organized as follows: In section "2," analytical model is derived. In section "3," a case study is presented. Finally, in section "2," concluding remarks are made.

2. Formulation

According to the plane elasticity theory, it is assumed that all the plane sections perpendicular to the central axis of cylinder, after applying pressure, remain flat and perpendicular to the central axis. The resultant deformations are symmetric with respect to the central axis and their values do not change along the length of the cylinder. Thus, the radial displacement u_r is only a function of radius r and both longitudinal stress σ_x and strain ε_x have constant values and normal stresses are principal stresses [22].

$$\sigma_\theta > \sigma_x > \sigma_r \tag{1}$$

The stress equation in the absence of body forces is defined by Eq. (2).

$$\frac{d\sigma_r}{dr} - \frac{\sigma_r - \sigma_\theta}{r} = 0 \tag{2}$$

Moreover, strain-displacement relation for axisymmetric case is defined as

$$\varepsilon_r = \frac{du_r}{dr} \quad , \quad \varepsilon_\theta = \frac{u_r}{r} \tag{3}$$

And for isotropic and heterogeneous material the stress is related to the strain as

$$\begin{Bmatrix} \sigma_r \\ \sigma_\theta \end{Bmatrix} = E(r) \begin{bmatrix} A & B \\ B & A \end{bmatrix} \begin{Bmatrix} \varepsilon_r \\ \varepsilon_\theta \end{Bmatrix} \tag{4}$$

where A and B are functions of Poisson's ratio and they are defined based on boundary conditions. In this paper, we assume that the Young's modulus is a power function of radius [23].

$$E(r) = E_i \left(\frac{r}{r_i} \right)^n = E_i \hat{r}^n \tag{5}$$

where E_i and r_i are Young's modulus and radius at inner side of the cylinder. n is heterogeneity constant of material.

Substituting Eqs. (3) and (4) in Eq. (2), one can obtain

$$r^2 \frac{d^2 u_r}{dr^2} + (n+1) r \frac{du_r}{dr} + \left(n\frac{B}{A} - 1 \right) u_r = 0 \tag{6}$$

Eq. (6) is a homogeneous, linear second order ODE (Cauchy-Euler equation), in which the roots of the characteristic polynomial

$$m^2 + nm + \left(n\frac{B}{A} - 1 \right) = 0 \tag{7}$$

could be real distinct, repeated and complex. The roots of the characteristic polynomial are

$$m_{1,2} = \frac{-n \pm \sqrt{\Delta}}{2} \quad , \quad \Delta = n^2 - 4\left(n\frac{B}{A} - 1 \right) \tag{8}$$

2.1. Real distinct roots

In this case, $\Delta > 0$, the general solution of Eq. (6) is:

$$u_r(r)=C_1 r^{m_1}+C_2 r^{m_2} \tag{9}$$

Using Eqs. (3) and (4), we get

$$\sigma(r)=E_i \hat{r}^n \begin{bmatrix} C_1(Am_1+B)r^{m_1-1}+ \\ C_2(Am_2+B)r^{m_2-1} \end{bmatrix} \tag{10}$$

The general equations of FGM cylindrical shells subjected to external and internal uniform pressure can be found in [6]. In this study, the derived equations for σ_r and σ_θ are simplified version of those equations as the outer cylinder is only subjected to internal pressure and the inner cylinder is subjected to external pressure. According to Fig. 1, we can consider the following loading conditions. It is assumed that both members have the same length.

Outer cylinder:

$$\sigma_r\Big|_{r=r_i=r_2}=-P \quad , \quad \sigma_r\Big|_{r=r_o=r_1}=0 \tag{11}$$

Inner cylinder:

$$\sigma_r\Big|_{r=r_i=r_3}=0 \quad , \quad \sigma_r\Big|_{r=r_o=r_2}=-P \tag{12}$$

Therefore, based on Eqs. (10), (11) and (12), the constants C_1 and C_2 can be obtained. Eqs. (13) and (14) show the constants C_1 and C_2 for outer and inner cylinders respectively.

$$\begin{aligned} C_1&=-\frac{Pk_1^{m_2}r_2^{(1-m_1)}}{E_2(Am_1+B)\left(k_1^{m_2}-k_1^{m_1}\right)} \\ C_2&=-\frac{Pk_1^{m_1}r_2^{(1-m_2)}}{E_2(Am_2+B)\left(k_1^{m_2}-k_1^{m_1}\right)} \end{aligned} \tag{13}$$

$$\begin{aligned} C_1&=-\frac{Pr_2}{E_3k_2^n r_3^{m_1}(Am_1+B)\left(k_2^{m_2}-k_2^{m_1}\right)} \\ C_2&=-\frac{Pr_2}{E_3k_2^n r_3^{m_2}(Am_2+B)\left(k_2^{m_1}-k_2^{m_2}\right)} \end{aligned} \tag{14}$$

where

$$k_1=\frac{r_1}{r_2}, \quad k_2=\frac{r_2}{r_3} \tag{15}$$

Substituting C_1 and C_2 in Eqs. (4) and (9), we have the following equations.

Outer cylinder:

$$\sigma_r=\frac{P\hat{r}^{n-1}}{k_1^{m_1}-k_1^{m_2}}\left(k_1^{m_2}\hat{r}^{m_1}-k_1^{m_1}\hat{r}^{m_2}\right) \tag{16}$$

$$\sigma_\theta=\frac{P\hat{r}^{n-1}}{k_1^{m_1}-k_1^{m_2}}\left(\frac{A+Bm_1}{Am_1+B}k_1^{m_2}\hat{r}^{m_1}-\frac{A+Bm_2}{Am_2+B}k_1^{m_1}\hat{r}^{m_2}\right) \tag{17}$$

$$u_r(r)\big|_{\mathrm{O}}=\frac{Pr_2}{E_2\left(k_1^{m_1}-k_1^{m_2}\right)}\left(\frac{k_1^{m_2}\hat{r}^{m_1}}{Am_1+B}-\frac{k_1^{m_1}\hat{r}^{m_2}}{Am_2+B}\right) \tag{18}$$

Inner cylinder:

$$\sigma_r=\frac{P}{\left(k_2^{m_2}-k_2^{m_1}\right)\hat{r}k_2^{n-1}}\left(\hat{r}^{n+m_1}-\hat{r}^{n+m_2}\right) \tag{19}$$

$$\sigma_\theta=\frac{P\hat{r}^{n-1}}{k_2^{m_2}-k_2^{m_1}}\left(\frac{A+Bm_1}{Am_1+B}\hat{r}^{n+m_1}-\frac{A+Bm_2}{Am_2+B}\hat{r}^{n+m_2}\right) \tag{20}$$

$$u_r(r)\big|_{\mathrm{I}}=\frac{Pr_2}{E_3k_2^n\left(k_2^{m_2}-k_2^{m_1}\right)}\left(\frac{\hat{r}^{m_1}}{Am_1+B}-\frac{\hat{r}^{m_2}}{Am_2+B}\right) \tag{21}$$

Now we should deal with the contact pressure P. Prior to assembly, the outer radius of the inner cylinder was larger than the inner radius of the outer cylinder by the radial interference δ. For Shrink-fitting the input of the problem is the radial interference, therefore the contact pressure is the result of δ.

$$\delta=u(r=r_2)\big|_{\mathrm{I}}+u(r=r_2)\big|_{\mathrm{O}} \tag{22}$$

Substituting Eqs. (18) and (21) into (22), the contact pressure can be obtained.

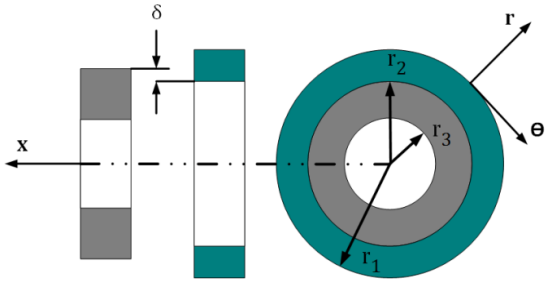

Fig 1. Schematic model of inner and outer cylinders and their notations

2.2. Repeated roots

In this case, Δ = 0, the general solution of Eq. (6) is

$$u_r(r)=(C_1+C_2 lnr)r^m \tag{23}$$

Following the same steps as section *2.1*, we achieve to the Eqs. (24) to (31).

Outer cylinder:

$$C_1=-\frac{P\left[A+(Am+B)lnr_1\right]}{E_2(Am+B)^2(lnk_1)r_2^{m-1}}$$
$$C_2=\frac{P}{E_2(Am+B)(lnk_1)r_2^{m-1}} \tag{24}$$

$$\sigma_r=-\frac{P\hat{r}^{(m+n-1)}}{lnk_1}\left(ln\frac{k_1}{\hat{r}}\right) \tag{25}$$

$$\sigma_\theta=\frac{P\hat{r}^{(m+n-1)}}{lnk_1}\left[\frac{B^2-A^2}{(Am+B)^2}-\frac{A+Bm}{Am+B}ln\frac{k_1}{\hat{r}}\right] \tag{26}$$

$$u_r(r)\big|_{\mathrm{O}}=\frac{Pr_2\hat{r}^m}{E_2(Am+B)lnk_1}\left(\frac{A}{Am+B}+ln\frac{k_1}{\hat{r}}\right) \tag{27}$$

Inner cylinder:

$$C_1=-\frac{P\left[A+(Am+B)lnr_3\right]}{E_3k_2^n(Am+B)^2(lnk_2)r_2^{m-1}}$$
$$C_2=\frac{P}{E_3k_2^n(Am+B)(lnk_2)r_2^{m-1}} \tag{28}$$

$$\sigma_r=-\frac{Pr_2\hat{r}^{(m+n-1)}}{k_2^{(n+m-1)}(Am+B)lnk_2}\begin{pmatrix}A+\\(Am+B)ln\hat{r}\end{pmatrix} \tag{29}$$

$$\sigma_\theta=\frac{P\hat{r}^{(m+n-1)}}{k_2^{(m+n-1)}(Am+B)lnk_2}\left[\frac{A^2+ABm}{Am+B}-(Am+B)ln\hat{r}-B\right] \tag{30}$$

$$u_r(r)\big|_{\mathrm{I}}=\frac{Pr_2\hat{r}^m}{E_3k_2^{(m+n)}(Am+B)lnk_2}\begin{pmatrix}\frac{A}{Am+B}\\-ln\hat{r}\end{pmatrix} \tag{31}$$

2.3. Complex roots

In this case, Δ < 0, so we have

$$m_{1,2}=z\pm iy$$
$$z=-\frac{n}{2}\quad,\quad y=\frac{\sqrt{-\Delta}}{2} \tag{32}$$

Therefore, the general solution of Eq. (6) is

$$u_r(r)=\left[C_1\cos(y lnr)+C_2\sin(y lnr)\right]r^z \tag{33}$$

Again following the same steps as section *2.1*, we achieve to the Eqs. (34) to (42).

Outer cylinder:

$$C_1=-\frac{Pr_2^{(1-z)}}{E_2D}\begin{bmatrix}(Az+B)\sin(y lnr_1)+\\Ay\cos(y lnr_1)\end{bmatrix}$$
$$C_2=\frac{Pr_2^{(1-z)}}{E_2D}\begin{bmatrix}(Az+B)\cos(y lnr_1)+\\Ay\sin(y lnr_1)\end{bmatrix} \tag{34}$$

where

$$D=\left[(Az+B)^2+A^2y^2\right]\sin(y lnk_1) \tag{35}$$

$$\sigma_r=-\frac{P\hat{r}^{(z+n-1)}}{\sin(y lnk_1)}\left(y ln\frac{k_1}{\hat{r}}\right) \tag{36}$$

$$\sigma_\theta=-\frac{P\hat{r}^{(z+n-1)}}{D}\left\{\left(A^2-B^2\right)y\cos\left(y ln\frac{k_1}{\hat{r}}\right)+\left[AB\left(z^2+y^2+1\right)+\left(A^2+B^2\right)z\right]\sin\left(y ln\frac{k_1}{\hat{r}}\right)\right\} \tag{37}$$

$$u_r(r)\big|_{\mathrm{O}}=\frac{Pr_2\hat{r}^z}{E_2D}\begin{bmatrix}(Az+B)\sin\left(y ln\frac{k_1}{\hat{r}}\right)+\\Ay\cos\left(y ln\frac{k_1}{\hat{r}}\right)\end{bmatrix} \tag{38}$$

Inner cylinder:

$$C_1=-\frac{Pr_2^{(1-z)}}{E_3k_2^nD}\begin{bmatrix}(Az+B)\sin(y lnr_3)+\\Ay\cos(y lnr_3)\end{bmatrix}$$
$$C_2=\frac{Pr_2^{(1-z)}}{E_3k_2^nD}\begin{bmatrix}(Az+B)\cos(y lnr_3)-\\Ay\sin(y lnr_3)\end{bmatrix} \tag{39}$$

where

$$D=\left[(Az+B)^2+A^2y^2\right]\sin(y lnk_2) \tag{40}$$

$$\sigma_r=-\frac{P\hat{r}^{(z+n-1)}}{\sin(y lnk_2)k_2^{(z+n-1)}}\sin(y ln\hat{r}) \tag{41}$$

$$\sigma_\theta=-\frac{P\hat{r}^{(z+n-1)}}{k_2^{(z+n-1)}D}\left\{\left(B^2-A^2\right)y\cos(y ln\hat{r})+\left[AB\left(z^2+y^2+1\right)+\left(A^2+B^2\right)z\right]\sin(y ln\hat{r})\right\} \tag{42}$$

$$u_r(r)\big|_{\mathrm{I}}=\frac{Pr_2\hat{r}^z}{E_3k_2^{(z+n)}D}\begin{bmatrix}(Az+B)\sin(y ln\hat{r})+\\Ay\cos(y ln\hat{r})\end{bmatrix} \tag{43}$$

3. Results and discussions

In this section as a case study, we consider two thick cylinders, which their characteristics are tabulated in table 1. Here we consider that for both of the cylinders the end boundary conditions are free-free. Eq. (44) shows the constants A and B for these boundary conditions. The analytical solution is carried out by writing an appropriated program in MATLAB.

$$\sigma_x = 0 \quad , \quad \varepsilon_x \neq 0$$
$$A = \frac{1}{1-\nu^2} \quad , \quad B = \frac{\nu}{1-\nu^2} \tag{44}$$

Figure 2 shows the distribution of the elasticity modulus along the cylinder's thickness. In this case study the inner surface of both cylinders is softer. Fig. 3 shows the distribution of radial stress along the thickness of both inner and outer cylinders. It can be seen from Fig. 3 that by increasing the heterogeneity constant *n* from -2 to 2 the radial stress increases, which means that the contact pressure value, is increasing too.

Figure 4 shows the distribution of the hoop stress along the thickness of both cylinders. It is obvious that the distribution of the hoop stress in both cylinders strongly depends on the value and sign of the heterogeneity constant *n*. According to Fig. 4 for negative values of heterogeneity constant *n*, the behavior of FG material is similar to homogeneous material. Next, we investigate the radial displacement in both cylinders. Fig.5 shows the radial displacement for the inner and outer cylinders. It can be concluded from Fig. 5 that as the heterogeneity constant *n* increases the radial displacement of the outer cylinder increases too. According to this Fig the behavior of the inner cylinder is complicated. For $n \leq 1$ the behavior of FG material is similar to the homogeneous material but for n>1 the behavior is completely different.

It is worth noting that in the case of homogeneous material (n=0) we can achieve to the conventional relations [22, 24] for hollow thick-walled cylinders under uniform internal and external pressure. Our present results for homogenous and isotropic material are in coincidence with reference [25].

Table 1. Geometrical and mechanical characteristics

Parameter	Value
E_i	200 GPa
r_1	60 mm
r_2	40 mm
r_3	20 mm
ν	0.3
δ	0.1 mm
n	$-2 \leq n \leq 2$

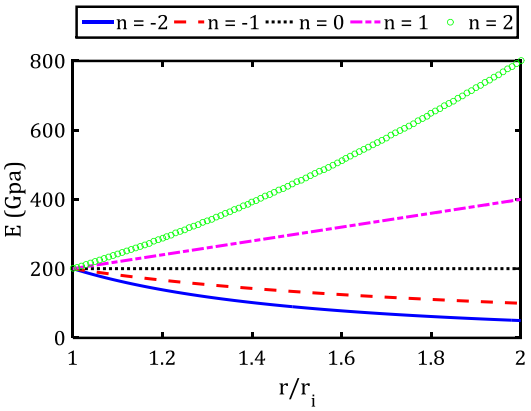

Fig 2. Distribution of elasticity modulus in the outer cylinder

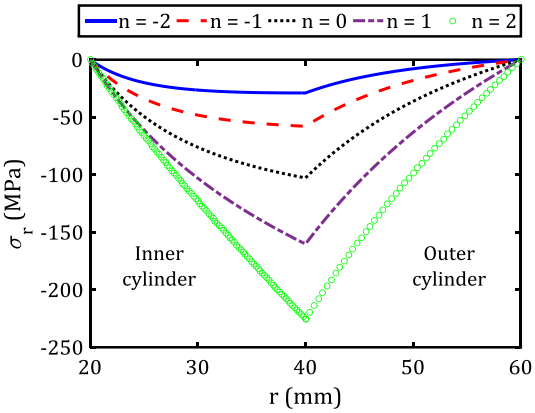

Fig 3. Continues distribution of radial stress

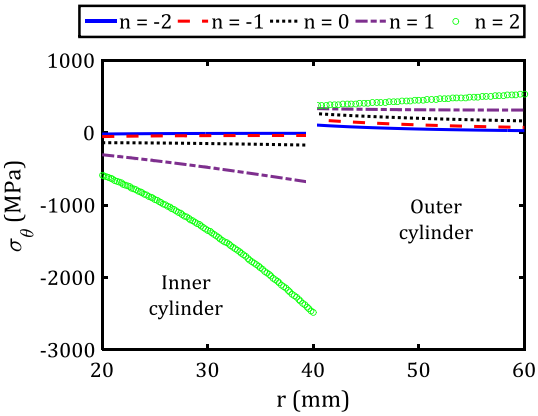

Fig 4. Continues distribution of hoop stress

4. Conclusions and Future Work

In this paper, based on plane elasticity theory, an analytical solution has been obtained for shrink-fitted axisymmetric hollow thick-walled cylindrical shells made of FG materials and the effects of compositional gradient exponent *n* of FG circular cylinder were investigated. The variation of FGM properties is supposed to be a power function along the thickness of cylinders. The results show that with increasing the softness (elastic module) of intersection area of fitted cylinders, the shrink-fit pressure reduced.

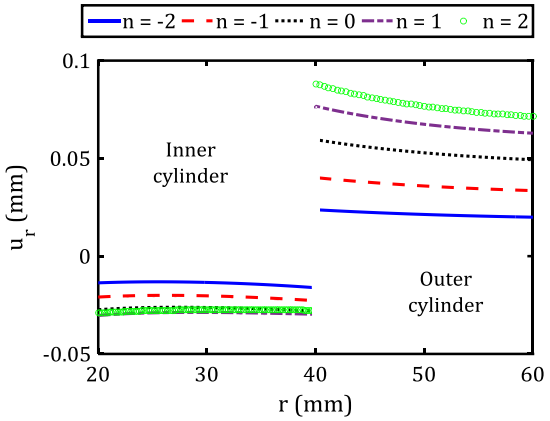

Fig 5. Continues distribution of radial displacement

Radial stress in inner surface of outer cylinder and outer surface of inner cylinder are equal to the shrink-fit pressure and in free internal and external surfaces of each cylinder are equal to zero. Hoop stress distribution is also dependent to the shrink-fit pressure. This stress has a variable direction and magnitude in cylinders. For *n*=-2,-1, 0 and 1 the hoop stress in inner and outer cylinders have values close together while for *n*=2 the hoop stress in inner cylinder is much larger than outer one. Future work will involve the effects of the temperature on the elastic behavior of shrink-fitted thick FGM cylinders.

References

[1] Damircheli M, Azadi M. Temperature and thickness effects on thermal and mechanical stresses of rotating FG-disks. *Journal of mechanical science and technology* 2011; 25(3): 827.

[2] Vaziri SA, Ghannad M, Bég OA. Exact thermoelastic analysis of a thick cylindrical functionally graded material shell under unsteady heating using first order shear deformation theory. *Heat Transfer—Asian Research* 2019.

[3] Azadi M. Free and forced vibration analysis of FG beam considering temperature dependency of material properties. *Journal of Mechanical Science and Technology* 2011; 25(1): 69-80.

[4] Zhang J. An elasticity solution for functionally graded thick-walled tube subjected to internal pressure. *International Journal of Mechanical Sciences* 2014; 89: 344-9.

[5] Ghannad M, Rahimi GH, Nejad MZ. Elastic analysis of pressurized thick cylindrical shells with variable thickness made of functionally graded materials. *Composites Part B: Engineering* 2013; 45(1): 388-96.

[6] Ghannad M, Nejad MZ. Complete elastic solution of pressurized thick cylindrical shells made of heterogeneous functionally graded materials. *Mechanics* 2012; 18(6): 640-9.

[7] Fukui Y, Yamanaka N. Elastic analysis for thick-walled tubes of functionally graded material subjected to internal pressure. *JSME international journal Ser 1, Solid mechanics, strength of materials* 1992; 35(4): 379-85.

[8] Xiang H, Shi Z, Zhang T. Elastic analyses of heterogeneous hollow cylinders. *Mechanics Research Communications* 2006; 33(5): 681-91.

[9] Zhao J, Wang J-X, Yu C, Tang S-Q, Yao J. Influence of radial interference on torque capacity of shrink-fit camshaft. *Advances in Mechanical Engineering* 2019; 11(4): 1687814018817640.

[10] Azad SK, Akış T. A Study of Shrink-Fitting for Optimal Design of Multi-Layer Composite Tubes Subjected to Internal and External Pressure. *Iranian Journal of Science and Technology, Transactions of Mechanical Engineering* 2019; 43(1): 451-67.

[11] Chu S, Jeong T, Jung E. Effect of radial interference on torque capacity of press-and shrink-fit gears. *International Journal of Automotive Technology* 2016; 17(5): 763-8.

[12] Booker J, Truman C. Measuring the coefficient of friction for use in shrink-fit calculations. *Experimental Techniques* 2011; 35(2): 7-13.

[13] Jahed H, Farshi B, Karimi M. Optimum autofrettage and shrink-fit combination in multi-layer cylinders. *Journal of Pressure Vessel Technology* 2006; 128(2): 196-200.

[14] Gexia Y, Hongzhao L, Zhongmin W. Optimum design for shrink-fit multi-layer vessels under ultrahigh pressure using different materials. *Chinese journal of mechanical engineering* 2010; (5): 582.

[15] Sharifi M, Arghavani J, Hematiyan M. An analytical solution for optimum design of shrink-fit multi-layer compound cylinders. *International Journal of Applied Mechanics* 2012; 4(04): 1250043.

[16] Timoshenko S. Strength of materials, part II. *Advanced theory and problems* 1941; 245.

[17] Lekhnitskii S. Theory of Elasticity of an Anisotropic Body (Moscow: MIR). Pleblishers; 1981.

[18] Koizumi M. FGM activities in Japan. *Composites Part B: Engineering* 1997; 28(1-2): 1-4.

[19] Pourasghar A, Moradi-Dastjerdi R, Yas M, Ghorbanpour Arani A, Kamarian S. Three-dimensional analysis of carbon nanotube-reinforced cylindrical shells with temperature-dependent properties under thermal environment. *Polymer Composites* 2018; 39(4): 1161-71.

[20] Arslan E, Mack W. Shrink fit with solid inclusion and functionally graded hub. *Composite Structures* 2015; 121: 217-24.
[21] Apatay T, Arslan E, Mack W. Elastic–plastic design of a rotating shrink fit with functionally graded hub. *Archive of Applied Mechanics* 2017; 87(11): 1829-43.
[22] Sadd MH. **Elasticity: theory, applications, and numerics**: Academic Press; 2009.
[23] Shi Z, Zhang T, Xiang H. Exact solutions of heterogeneous elastic hollow cylinders. *Composite structures* 2007; 79(1): 140-7.
[24] Shigley JE. **Shigley's mechanical engineering design**: Tata McGraw-Hill Education; 2011.
[25] Ugural AC, Fenster SK. **Advanced mechanics of materials and applied elasticity**: Pearson Education; 2011.